

# Spatial Resolution of Single-Cell Exocytosis by Microwell-Based Individually Addressable Thin Film Ultramicroelectrode Arrays

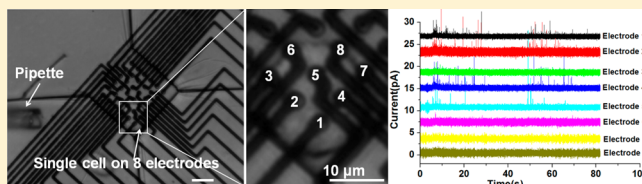
Jun Wang,<sup>†,‡</sup> Raphaël Trouillon,<sup>†</sup> Johan Dunevall,<sup>‡</sup> and Andrew G. Ewing<sup>\*,†,‡</sup>

<sup>†</sup>Department of Chemistry and Molecular Biology, University of Gothenburg, Kemivägen 10, 41296 Gothenburg, Sweden

<sup>‡</sup>Department of Chemical and Biological Engineering, Chalmers University of Technology, Kemivägen 10, 41296 Gothenburg, Sweden

## S Supporting Information

**ABSTRACT:** We report the fabrication and characterization of microwell-based individually addressable microelectrode arrays (MEAs) and their application to spatially and temporally resolved detection of neurotransmitter release across a single pheochromocytoma (PC12) cell. The microwell-based MEAs consist of 16 4- $\mu\text{m}$ -width square ultramicroelectrodes, 25 3- $\mu\text{m}$ -width square ultramicroelectrodes, or 36 2- $\mu\text{m}$ -width square ultramicroelectrodes, all inside a 40  $\times$  40  $\mu\text{m}$  square SU-8 microwell. MEAs were fabricated on glass substrates by photolithography, thin film deposition, and reactive ion etching. The ultramicroelectrodes in each MEA are tightly defined in a 30  $\times$  30  $\mu\text{m}$  square area, which is further encased inside the SU-8 microwell. With this method, we demonstrate that these microelectrodes are stable, reproducible, and demonstrate good electrochemical properties using cyclic voltammetry. Effective targeting and culture of a single cell is achieved by combining cell-sized microwell trapping and cell-picking micropipette techniques. The surface of the microelectrodes in the MEA was coated with collagen IV to promote cell adhesion and further single-cell culture, as good adhesion between the cell membrane and the electrode surface is critical for the quality of the measurements. Imaging the spatial distribution of exocytosis at the surface of a single PC12 cell has also been demonstrated with this system. Exocytotic signals have been successfully recorded from eight independent 2- $\mu\text{m}$ -wide ultramicroelectrodes from a single PC12 cell showing that the subcellular heterogeneity in single-cell exocytosis can be precisely analyzed with these microwell-based MEAs.



Neurons and other cells are heterogeneous systems owing to specialized protein machineries and lipid domains leading to spatial variations in the cell membranes, nature, and location of exocytotic release.<sup>1,2</sup> Several kinds of well-established cell models for neuron cell exocytosis study have been widely used for this kind of study.<sup>3</sup> For example, the distribution of exocytotic activity has been found to be spatially heterogeneous at the surface of the well-established neuronal cell model, including the adrenal chromaffin cell<sup>4–6</sup> and dopamine-secreting pheochromocytoma (PC12) cell line,<sup>7–9</sup> resulting in locations (hot spots) where neurotransmitters are released more frequently. This subcellular heterogeneity across a single cell thus motivated the design of MEA devices capable of resolving the spatial variation of exocytosis across a single cell. Different parts of the membrane on the same cell or in the intact brain with different exocytosis activity (hot spots or cold spots) have been confirmed by use of these MEA devices.<sup>10,11</sup> In related experiments *in vivo*, the Michael group reported a method of constructing two or four individually addressable carbon ultramicroelectrodes (radii  $\approx$  1  $\mu\text{m}$ ) separated by a distance of  $\approx$  15  $\mu\text{m}$ .<sup>12</sup> Each carbon fiber was etched into a sharp tip and then electrically isolated by coating the tip with poly(allylphenol). These individual electrochemical arrays were used to simultaneously probe dopamine release in the brain at multiple spatially separate sites. Thus, the spatial resolution

across single-cell membranes or high-throughput sensing of multiple analytes, or the study of signal transmission in cell networks can all be achieved with these MEAs. However, most of these kinds of MEAs are used to collect vesicular release information from the apical pole of single cells.

Recent advances in the design of new thin film MEAs by Micro-Electro-Mechanical System (MEMS) techniques have led to MEAs with a number of properties that make them ideally suited to the analysis of biological systems from the basal side of the cell. This technology involves the use of successive steps of photolithography, thin film metal deposition, and reactive ion etching to reproducibly fabricate individually addressable MEAs for single-cell experiments.<sup>13–18</sup> However, few papers have described individually addressable MEAs with individual microelectrodes smaller than 5  $\mu\text{m}$ ,<sup>19,20</sup> the typical size of the carbon fiber microelectrode that are used for the detection of easily oxidizable neurochemicals from single cells. Furthermore, most of these papers have reported single-cell trapping or detection at a single electrode. The development of MEAs with tightly packed microelectrodes small enough to allow quantitative measurement of released molecules from

Received: January 31, 2014

Accepted: April 8, 2014

Published: April 8, 2014

exocytotic hot spots distributed on the surface of a single cell would be very attractive for amperometric measurements. We recently reported the fabrication of thin-film MEAs and used these to electrochemically image the exocytotic release of dopamine from cells clusters. These were 4 by 4 MEAs containing 4  $\mu\text{m}$  width microelectrodes.<sup>21</sup> However, because one of the unique properties of tightly packed microelectrodes in MEA methods is to investigate spatial heterogeneity of these exocytotic events at the single-cell level, combining other techniques to precisely attach single cells and to culture single cells on the surface of MEAs is of interest. Additionally, development of smaller electrodes is important for studies of single-cell heterogeneity and spatial resolution. Recently, advances in lab-on-chip techniques have given rise to integrated microfluidic devices and systems. Capture and/or analysis of single cells with these lab-on-a-chip approaches by several single-cell manipulation strategies have been carried out, including microwell-based docking, electrokinetic or hydrodynamic single-cell focusing, and injection techniques, etc.<sup>22–26</sup>

In this paper, we combine lab-on-chip techniques (microwell) to precisely trap single cells on the surface of MEAs with up to 36 electrodes as small as 2  $\mu\text{m}$ . We present the fabrication, characterization, and application of this system to the analysis of cell exocytosis by use of a 40  $\times$  40  $\mu\text{m}$ -sized square microwell for single-cell trapping and single-cell culturing on the surface of multiple microelectrodes. These microwell-based MEA combinations feature sizes compatible with individual neuronal or neuronlike cells, thus offering subcellular resolution of exocytotic imaging. Effective targeting and culture of single cells in the microwell are achieved by combining cell-sized microwell trap and micropipet picking techniques. The surface of the microelectrodes in the MEAs has been coated with collagen IV to promote cell adhesion. Steady state voltammetry has been applied to study the activity of these microelectrodes. The spatial resolution of single-cell exocytosis has been studied by use of multiple 2  $\mu\text{m}$  microelectrodes simultaneously from these microwell-based 6  $\times$  6 MEAs.

## EXPERIMENTAL SECTION

**Fabrication of the Microwell-Based MEAs.** Figure 1 (panels A, B, and C) show three kinds of MEAs consisting of

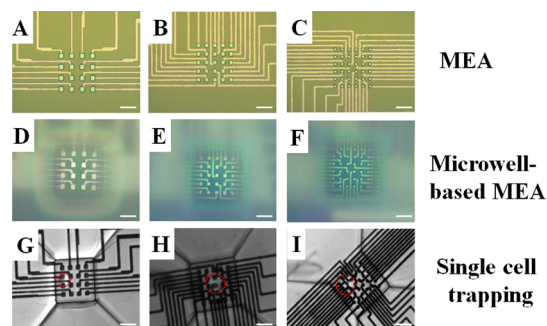


**Figure 1.** Optical micrographs of three kinds of MEAs, three kinds of microwell-based MEAs, and single-cells trapping in three kinds of microwell-based MEAs. (A–C) show MEAs consisting of 16, 25, and 36 microelectrodes, respectively (scale bars are 10  $\mu\text{m}$ ); (D–F) show the SU-8 microwells on top of 4 by 4, 5 by 5, and 6 by 6 MEAs (scale bars are 10  $\mu\text{m}$ ); and (G–I) show examples of trapped single cells (identified in red dotted circles) in microwell-based MEAs showing 16, 25, 36 microelectrodes, respectively (scale bars are 10  $\mu\text{m}$ ).

16, 25, 36 square microelectrodes with respective widths of 4, 3, and 2  $\mu\text{m}$ . As previously described,<sup>21</sup> Ti/Pt (5 nm/45 nm) were deposited on glass wafer by electron-beam evaporator using lift-off techniques, and next, an insulation layer  $\text{Si}_3\text{N}_4$  film (425 nm) was deposited and then etched by  $\text{CF}_4$  to form these MEAs with recessed microelectrodes. Here we only emphasize how to fabricate microwells on top of MEAs; we used the thick photoresist SU-8 2035 (MicroChem) to fabricate microwells on top of MEAs, glass wafers with MEAs were spin-coated at 4000 rpm for 1 min to yield a film thickness of about 25  $\mu\text{m}$ . Then the wafer was baked at 65  $^\circ\text{C}$  for 2 min, 95  $^\circ\text{C}$  for 6 min, and 65  $^\circ\text{C}$  for 2 min on a hot plate. The 40  $\times$  40  $\mu\text{m}$  square microwells pattern was defined on top of the MEAs by UV lithography (KS MA6, Suss MicroTec) with a chrome mask showing the microwell design. After UV exposure, it was subsequently baked at 65  $^\circ\text{C}$  for 2 min, 95  $^\circ\text{C}$  for 6 min, and 65  $^\circ\text{C}$  for 2 min on a hot plate. It was then developed with SU-8 developer for 2 min with a mild shake. Then the device was baked at 175  $^\circ\text{C}$  for 10 min on a hot plate, finally forming a 40  $\times$  40  $\mu\text{m}$  size microwell on top of the three kinds of MEAs (Figure 1, panels D, E, and F).

Subsequently, a polydimethylsiloxane (PDMS) chamber (2  $\times$  3 cm) was prepared and bonded to this SU-8 film on the glass wafer for the cell-medium reservoir and for cell culture. Electrical contact was achieved by manually placing connection pads on to the glass wafer from the multiple pin heads of socket connectors (ELFA, Gothenburg) by using silver paste 4922N (Dupont). The microwell-based device was then baked at 100  $^\circ\text{C}$  overnight, and the final device was obtained with the microwells on top of MEAs shown in Figure S1 of the Supporting Information.

**Collagen Coating and Single-Cell Culture on Top of Microwell-Based MEAs.** Mouse collagen IV (BD Biosciences, Bedford, MA BD chemicals, stock solution 1 mg/mL) was used for coating the surface area of the PDMS chamber. A cell was then seeded in the SU-8 microwell on top of a MEA, and the cell medium was added in the PDMS well on the glass wafer for cell culture. Here we incubate about 2 mL of collagen IV solution (1  $\mu\text{g}/\text{mL}$ ) in this PDMS well for 8 h. Then the PDMS well was washed three times with 1 $\times$  sterile Dulbecco's phosphate-buffered saline without calcium and magnesium. Cells were then deposited into the PDMS chamber on the MEA device by adding 2 mL of PC12 cell suspension (about 10<sup>4</sup> cells/mL). After loading cells on the PDMS chamber, a glass micropipet (tip diameter about 5  $\mu\text{m}$ ) was used to pick up an individual cell and place it into the microwell. Then the device was placed in the sterile incubator for cell culture. Briefly, the cells were maintained and cultured as previously described.<sup>21,27</sup> For stimulated single-cell exocytosis experiments, single cells were grown in the well on the MEAs for 1–2 days before experiments, and the cell media was replaced every day.

**Electrochemical Imaging of Single-Cell Exocytosis.** All cell experiments were performed at 37  $\pm$  1  $^\circ\text{C}$ . Single-cell exocytosis was recorded from multiple microelectrodes by use of a Triton<sup>+</sup>48-channel patch clamp amplifier (Tecella, Foothill Ranch, CA), which was placed in a Faraday cage. Optical images of microwell-based MEA experiments were obtained from a  $\times$  40 objective (0.65 n.a.) with an inverted microscope (IX71, Olympus). The amperometric current traces were processed using IgorPro 6.21 software (Wavemetrics, USA), as David Sulzer's group reported.<sup>28</sup> After current events were detected with the software, current traces and current events

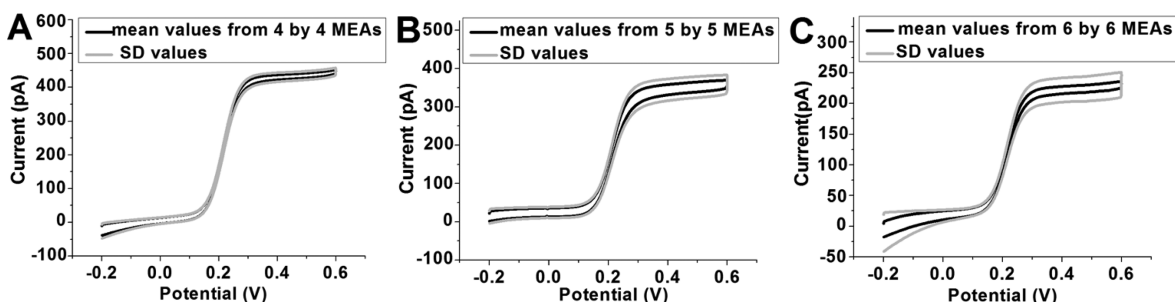


**Figure 2.** Electrochemical characterization of the microelectrodes in three kinds of microwell-based MEAs featuring (A) 4 by 4 MEAs, (B) 5 by 5 MEAs, and (C) 6 by 6 MEAs. The cyclic voltammograms (scan rate: 20 mV/s) were obtained in 1 mM FcMeOH in PBS buffer (pH 7.4) by sequentially applying potential to each microelectrode. The black curves show the average voltammogram obtained from the signals measured at each microelectrode of the MEA, and the gray curves show the corresponding standard deviation (SD) values (16 electrode MEA,  $n = 16$ ; 25 electrode MEA,  $n = 25$ ; and 36 electrode MEA,  $n = 36$ ).

were checked manually to reject false positive signals. False positives (about 5%) that were recognized by the software were manually rejected and the fitting of the peak parameters was adjusted. Other experimental details were performed as previously described.<sup>21,29</sup>

## RESULTS AND DISCUSSION

**Microwell-based MEA device characterization.** Figure 1 (panels A–C) show optical images of three kinds of MEAs containing different size of microelectrodes. Figure 1 (panels D–F) show each type of MEA encased into a  $40 \times 40 \mu\text{m}$  SU-8 microwell, which can be used to trap a single cell on top of the array. SEM pictures of three kinds of microwell-based MEAs are also shown in Figure S1 of the Supporting Information. These pictures clearly show the whole MEA containing tightly packed multiple microelectrodes tightly defined in a  $40 \times 40 \mu\text{m}$  square SU-8 microwell area, which is potentially useful to trap a single cell. The success rate for the fabrication of microwell-based MEAs is quite high, the average success rate can be 95% for all MEAs, although for MEAs with the smallest microelectrodes ( $2 \mu\text{m}$  width), the success rate is lower, and for MEAs with larger microelectrodes ( $5 \mu\text{m}$  width) the success rate is higher. When cells were placed in the PDMS chamber for cell seeding, we manually placed a single cell in this  $40 \times 40 \mu\text{m}$  SU-8 microwell by using a micropipet (tip diameter about  $5 \mu\text{m}$ ) and a micromanipulator. Because of the collagen IV coated surface, single cells adhere on the surface of the MEA in the well, when this device is placed in a cell-culture incubator for 1 or 2 days. The success rate for trapping single cells is approximately 80%, which is comparable to other single-cell trapping approaches.<sup>22</sup> Figure 1 (panels G–I) show examples of single cells (each cell is identified with a red dotted circle) successfully trapped inside microwells for the three different kinds of MEAs. Since single cells are targeted to the electrodes without nearby extraneous cells, individual cell responses can be unambiguously recorded. Vigorous solution exchange can be carried out without displacing cells from the electrodes. After each cell culture and exocytosis experiment, the cell chamber was incubated with 2% SDS, rinsed with deionized water three times, then rinsed with acetone, isopropanol, and deionized water, blown dry with nitrogen, and then cleaned with an oxygen plasma. The cell culture, cell exocytosis experiment, and cleaning steps with this microwell-based MEA device have been carried out about 20 times (several months) without significant degradation of the electrochemical performance (Figure S2 of the Supporting Information).

We then characterized the electrochemical performance of microelectrodes in these three kinds of microwell-based MEAs. Cyclic voltammograms of 1 mM ferrocenemethanol (FcMeOH) were obtained for these three kinds of microwell-based MEAs by sequentially applying potential to each microelectrode, as shown in Figure 2. Steady-state voltammetric behavior is obtained for these three kinds of microwell-based MEAs; the voltammetric waves are well-defined having sigmoidal shape at this scan rate, and this agrees well with the microelectrode theory. The diffusion-limited current ( $i_{\text{dl}}$ ) was measured for each electrode in different kinds of microwell-based MEAs, and the averaged values for the 4 by 4, 5 by 5, or 6 by 6 microwell-based MEAs are shown in Table 1.

**Table 1.** Experimental ( $n = 6$  microelectrode arrays) and Calculated Diffusion Limited Current  $i_{\text{dl}}$  value at a Recessed Disk Electrode for Three Kinds of Microwell-Based MEAs Assuming a Recess Depth of 375 nm

	4 by 4 MEA	5 by 5 MEA	6 By 6 MEA
width ( $\mu\text{m}$ )	4	3	2
experimental $i_{\text{dl}}$ (pA) (mean $\pm$ SD)	$437.2 \pm 6.3$	$356.5 \pm 9.3$	$215.3 \pm 11.5$
calculated $i_{\text{dl}}$ (pA) (mean $\pm$ SD)	485.9	342.7	205.7

The microwell-based MEA device presented here has microelectrodes with a recessed depth of 375 nm, possibly restricting the diffusion of analytes to the microelectrode surface. The theoretical value for  $i_{\text{dl}}$  at cathodic potentials for a single, recessed, microdisk electrode is given by

$$i_{\text{dl}} = 4\pi r^2 nFD \frac{C}{\pi r + 4h} \quad (1)$$

where  $n$  is the number of electrons transferred in the reaction,  $F$  is the Faraday constant,  $C$  is concentration of analyte,  $D$  is the diffusion coefficient,  $r$  is the radius of microelectrode, and  $h$  is the depth of the recess.<sup>30</sup> This equation was used here to approximate the measured current at a recessed square electrode for geometric values compatible with the geometry of our system (we approximate our square electrode as a disk electrode with  $r = 1/2$  width of the square electrode, which were 2, 1.5, or  $1 \mu\text{m}$ ;  $h = 375 \text{ nm}$ ). The calculated theoretical  $i_{\text{dl}}$  values, for each kind of recessed MEA, are presented in Table 1. The calculated  $i_{\text{dl}}$  values (485.9 pA for a single microelectrode from a 4 by 4 microwell-based MEA; 342.7 pA for a single microelectrode from a 5 by 5 microwell-based MEA; 205.7 pA



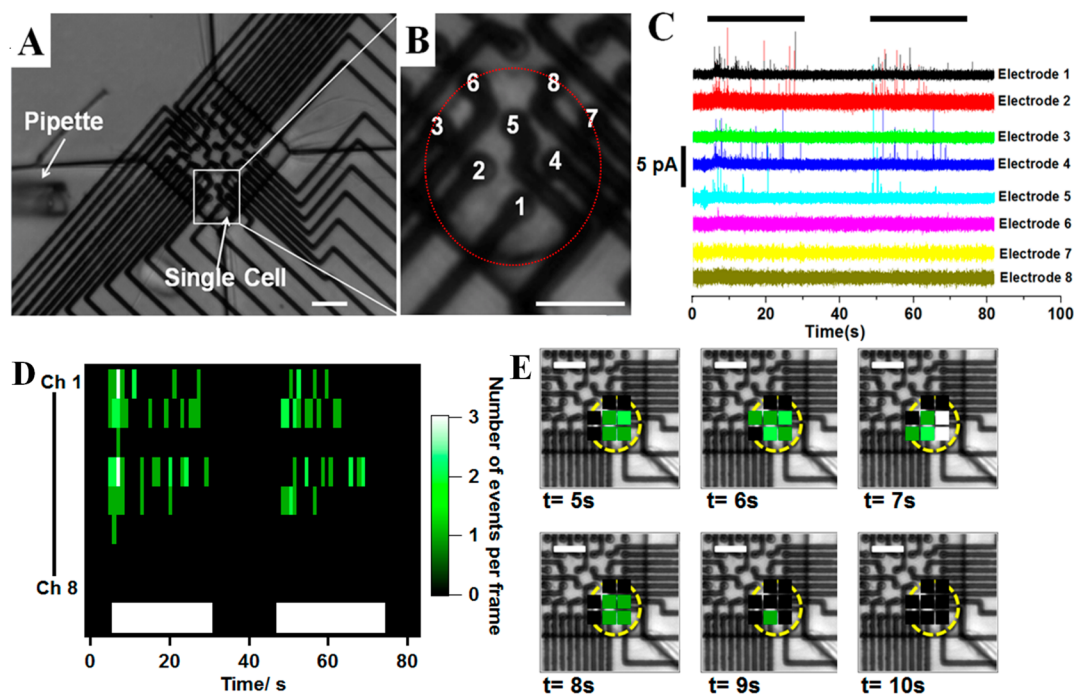


**Figure 3.** Electrochemical imaging of a single PC12 cell covering multiple microelectrodes in the microwell-based 6 by 6 MEA. (A) Micrograph of the setup, showing the 36-electrode array partially covered by a single PC12 cell (scale bar: 10  $\mu\text{m}$ ); (B) expanded view of the electrode array showing a single cell identified in a red dotted circle and the labeling of the electrodes (scale bar: 10  $\mu\text{m}$ ); (C) representative amperometric traces of exocytotic release from a PC12 cell recorded at 8 electrodes for 25 s stimulations of the cell (the stimulations are indicated by the black bars); (D) frequency color plots showing the release frequency obtained for each channel, for 1 s frames. The white pixels show the duration of the  $\text{K}^+$  stimulation; (E) electrochemical imaging of the release frequency at each of the 8 electrodes (scale bar: 10  $\mu\text{m}$ ).

for a single microelectrode from a 6 by 6 microwell-based MEA) in these three kinds of microwell-based MEAs agree well with the experimental values (437.2 pA for a single microelectrode from a 4 by 4 microwell-based MEA; 356.5 pA for a single microelectrode from a 5 by 5 microwell-based MEA; and 215.3 pA for a single microelectrode from a 6 by 6 microwell-based MEA). The agreement is within 10%, suggesting that perhaps the working area is slightly different as expected or the approximation of our square microelectrodes by a microdisk electrode is not perfect. Figure S3 of the Supporting Information shows cyclic voltammograms of 1 mM ferrocene-methanol (FcMeOH) for these three kinds of microwell-based MEAs by simultaneously applying potential to 8 neighboring microelectrodes. The experimental  $i_{\text{dl}}$  values obtained by simultaneously applying potential to each microelectrode are much lower than calculated or experimental  $i_{\text{dl}}$  values obtained by sequentially applying a potential to each microelectrode of three kinds of microwell-based MEAs. The lower  $i_{\text{dl}}$  values apparently result from diffusional cross talk induced by the short interelectrode distance. The limiting currents from 4 by 4 MEA microelectrodes or 5 by 5 MEA microelectrodes obtained by simultaneously applying potential to all microelectrodes (Figure S3 of the Supporting Information) are  $\sim 40\%$  smaller than the limiting current of each individually measured microelectrode (Figure 2). The limiting current from 6 by 6 MEA microelectrodes obtained by simultaneously applying potential to microelectrodes (Figure S3 of the Supporting Information) is  $\sim 22\%$  smaller than the limiting current at individually measured microelectrodes (Figure 2). These results clearly show the overlap of the depletion layers between multiple electrodes when used simultaneously. Previous theories have also shown that overlap in the diffusion fields

at inlaid neighboring electrodes can reduce the mass transport to the electrode, thus leading to lower measured  $i_{\text{dl}}$  in comparison to its theoretical value.<sup>8,31,32</sup>

**Electrochemical Imaging of Release at a Single PC12 Cell.** Compared to other MEAs, the smaller microelectrodes in the 6 by 6 MEAs are more useful for the study of single-cell exocytosis. This is because more electrodes of smaller size can be used to cover a single cell, and higher spatial resolution can be obtained. Here, we mainly focus on the study of single-cell exocytosis studied with the microwell-based 6 by 6 MEAs. Electrochemical imaging of single-cell exocytosis by multiple microelectrodes is shown in Figure 3. A single cell is trapped and cultured on the surface of a 6 by 6 microwell-based MEA containing 36 microelectrodes (Figure 3A). This single cell identified with a red-dotted circle covered about 8 electrodes. The electrode number, which will be used further below, is also shown in Figure 3B. An advantage of the 36-electrode array is that we can image across a single-cell membrane with more microelectrodes to confirm the active exocytosis location on the cell. Electrodes 1–8 are covered by the cell in this example and exocytotic events are observed at these electrodes upon stimulation (Figure 3C). Representative amperometric traces of exocytotic release from a PC12 cell are shown for 8 electrodes following 25 s stimulations of the cell. A 4 s current trace (Figure S4 of the Supporting Information) expanded from Figure 3C shows the noise level at different microelectrodes (noise level is 1–2 pA). Different noise levels are observed for different microelectrodes in the same MEA and might result from the connection between the socket connector and the contact pad of the MEAs on the glass wafer, where this is done manually using silver paste. The contact resistance between the socket connectors and different microelectrodes might be

slightly different. The results also show fewer current transients or exocytotic events at electrodes E3 and E6, which confirms the heterogeneity of single-cell exocytosis and that PC12 cells contain active zones of vesicle fusion and release.

Electrochemical imaging of exocytosis at a PC12 cell, similar to that shown in Figure 3 (panels A–C), is presented in Figure 3 (panels D and E). Color plots of the release frequency at each microelectrode (1 s time bins) in this array are shown in Figure 3D. Higher release frequency is represented by light green and white color, whereas lower release frequency is represented by dark green and black colors. Time variations in release frequency at each microelectrode are also shown in color plots (Figure 3E) based on the optical image of a single cell covering multiple microelectrodes. Each color square is an independent electrode from a 6 by 6 MEA. The pictures shown here are focused on two stimulations performed during the course of the experiment. The spots showing high release frequencies can be easily identified from this graphical representation, which shows the spatial release of dopamine and the exocytotic activity in different microelectrodes or different parts of the membrane. A movie built from the data presented in this figure is available as Supporting Information (see ac500443q\_si\_002.avi). The subcellular spatial heterogeneity of exocytosis can be observed in Figure 3. The location of “hot” release spots has been found to vary with time across the surface of a single cell. There are different numbers of vesicle events detected at different stimulation time at the same electrode (see Figure S5 of the Supporting Information). The microwell-based MEA allows detection of the localized membrane function in terms of single-cell exocytosis. Furthermore, as shown on the frequency plots (Figure 3, panels D and E), the electrodes showing the highest release frequency are also the ones located over electrodes fully covered by the cell (electrodes 1, 2, 4, and 5). Fewer release events were measured in electrodes 3 and 6, and no release events were detected by electrodes 7 and 8, which are partially covered by the cell. Thus, the incomplete cell adhesion over the electrode might also affect the detection threshold.

**Simultaneous Exocytotic Events.** The incidence of concurrent events on the same cell can be examined with the 6 by 6 MEA. When more than one event occurs simultaneously, it is challenging to resolve them using a single microelectrode. In the absence of spatial resolution, these events will overlap and result in a large, broad current spike. Simultaneous, parallel recordings using multiple microelectrodes allow these events to be resolved based on spatial identification. Figure 4 shows a 0.5

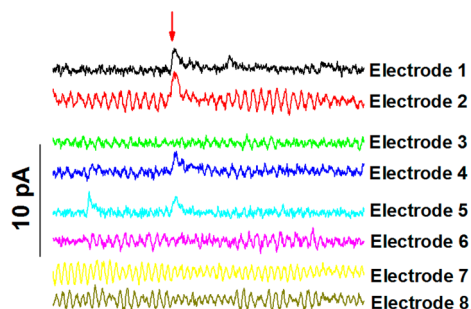


**Figure 4.** A 0.5 s time period of the exocytotic response of a PC12 cell after  $K^+$  stimulation showing the detection of simultaneous concurrent spikes at different locations on the same cell. Red arrow indicates these events.

s amperometric recording at a single PC12 cell using a 6 by 6 MEA. The red arrows indicate four different exocytotic events are detected from electrodes 1, 2, 4, and 5. The events are extremely similar temporally, thus with only one larger electrode they would form a single large, broader current spike. Although rare, these overlapping events can be spatially resolved by this 6 by 6 MEA. The amount of neurotransmitter molecules released associated with each of these concurrent spikes is reported in Table 2. Each of these values, measured at

**Table 2.** Exocytotic Parameters Obtained for the Concurrent Spikes of Figure 4, at Different Electrodes<sup>a</sup>

	E1	E2	E4	E5	total
$N$ ( $\times 10^3$ molecules)	92	93	87	52	$91 \pm 4.1$
$i_p$ (pA)	2.1	2.7	2.0	2.1	$2.8 \pm 0.2$
$t_{fall}$ (ms)	9.3	3.1	9.1	6.9	$5.9 \pm 0.3$

<sup>a</sup>The values obtained for the total population of events, over the 8 electrodes, is presented in the column “total” (143 events, average  $\pm$  SEM).

the four independent electrodes, is in agreement with the mean amount of  $N$  for all the events recorded during the course of the experiment. This observation is in agreement with the possibility that these concurrent events are produced by different vesicles simultaneously released at different membrane regions in the single cell and detected at the same time by MEA. A previous analysis and theory of electrochemical detection of single exocytotic events at carbon microelectrodes showed that, for an event whose features correspond to the mean of the exocytotic parameters obtained from events recorded at a typical PC12 cell, the sensing capability of the electrode decreases rapidly when the fusion event is further than about 700 nm away from the electrode edge.<sup>33</sup> However, as these four electrodes are adjacent, and for huge vesicles or vesicle clusters in PC12 cells, it is possible that an event might be detected more than 700 nm. If these peaks arise from a single large event detected simultaneously at four different locations then by summing the  $N$  presented in Table 2 for the 4 concurrent events,  $324 \times 10^3$  molecules would have been released in total. This would correspond to a very large vesicle from a PC12 cell. From Figure 3C, we observed about  $\sim 10\%$  concurrent events occur in two neighboring electrodes in our MEAs, and  $\sim 1\%$  concurrent events occur in over two neighboring electrodes, we also observed that the concurrent events occurring between E1 and E5 or E1 and E4 are much fewer than the concurrent events between E1 and E2, E2 and E5, or E4 and E5, which may be because the interelectrode distances between E1 and E4 or E1 and E5 are larger than the others, and we did not observe concurrent events occurring in non-neighboring electrodes such as E1 and E3 or E1 and E6. It is possible that some events are very large and give rise to this behavior, or it is possible that distinct concurrent events are more likely to take place at adjacent places on a cell. We cannot discriminate these possibilities with the current methods.

## CONCLUSIONS

We have fabricated microwell-based MEAs that can be used to spatially probe chemical changes in tight spaces, such as studying exocytosis from different regions of single-cell surfaces. These arrays are on the order of 40  $\mu\text{m}$  across and are geometrically well-defined. Additionally, the MEAs have well-defined electrochemical behavior, and up to 36 microelectrodes

can be individually addressed. We used these microwell-based MEAs for high-throughput amperometric measurement of quantal exocytosis from individual cells cultured in microwells without the need for microfluidic forces to be applied to the cell. The 6 by 6 MEA has been used to simultaneously electrochemically monitor exocytotic events from different surface regions of a single PC12 cell showing subcellular heterogeneity with 2  $\mu\text{m}$  resolution. Concurrent exocytotic events under different microelectrodes have been resolved using these microwell-based MEAs.

## ■ ASSOCIATED CONTENT

### ■ Supporting Information

Additional information as noted in text. This material is available free of charge via the Internet at <http://pubs.acs.org>.

## ■ AUTHOR INFORMATION

### Corresponding Author

\*E-mail: [andrew.ewing@chem.gu.se](mailto:andrew.ewing@chem.gu.se).

### Notes

The authors declare no competing financial interest.

## ■ ACKNOWLEDGMENTS

The European Research Council (Advanced Grant), Knut and Alice Wallenberg Foundation, the Swedish Research Council (VR), and the National Institutes of Health are acknowledged for financial support.

## ■ REFERENCES

- (1) Walch-Solimena, C.; Jahn, R.; Sudhof, T. C. *Curr. Opin. Neurobiol.* **1993**, *3*, 329–336.
- (2) Kelly, R. B. *Neuron* **1988**, *1*, 431–438.
- (3) Greene, G. A.; Rein, G. *Brain Res.* **1977**, *129*, 247–263.
- (4) Monck, J. R.; Robinson, I. M.; Escobar, A. L.; Vergara, J. L.; Fernandez, J. M. *Biophys. J.* **1994**, *67* (2), 505–514.
- (5) Schroeder, T. J.; Jankowski, J. A.; Senyshyn, J.; Holz, R. W.; Wightman, R. M. *J. Biol. Chem.* **1994**, *269*, 17215–17220.
- (6) Robinson, I. M.; Finnegan, J. M.; Monck, J. R.; Wightman, R. M.; Fernandez, J. M. *Proc. Natl. Acad. Sci. U.S.A.* **1995**, *92*, 2474–2478.
- (7) Kozminski, K. D.; Gutman, D. A.; Davila, V.; Sulzer, D.; Ewing, A. G. *Anal. Chem.* **1998**, *70*, 3123–3130.
- (8) Zhang, B.; Adams, K. L.; Lubner, S. J.; Eves, D. J.; Heien, M. L.; Ewing, A. G. *Anal. Chem.* **2008**, *80*, 1394–1400.
- (9) Lin, Y.; Trouillon, R.; Svensson, M. I.; Keighron, J. D.; Cans, A.-S.; Ewing, A. G. *Anal. Chem.* **2012**, *84*, 2949–2954.
- (10) Droge, M. H.; Gross, G. W.; Hightower, M. G.; Csisny, L. E. *J. Neurosci.* **1986**, *6*, 1583.
- (11) Maher, M. P.; Pine, J.; Wright, J.; Tai, Y. C. *J. Neurosci. Methods* **1999**, *87*, 45.
- (12) Dressman, S. F.; Peters, J. L.; Michael, A. C. *J. Neurosci. Methods* **2002**, *119*, 75.
- (13) Carabelli, V.; Gosso, S.; Marcantoni, A.; Xu, Y.; Colombo, E.; Gao, Z.; Vittone, E.; Kohn, E.; Pasquarelli, A.; Carbone, E. *Biosens. Bioelectron.* **2010**, *26*, 92–98.
- (14) Sun, X. H.; Gillis, K. D. *Anal. Chem.* **2006**, *78*, 2521–2525.
- (15) Chen, X. H.; Gao, Y. F.; Hossain, M.; Gangopadhyay, S.; Gillis, K. D. *Lab Chip* **2008**, *8*, 161–169.
- (16) Dittami, G. M.; Rabbitt, R. D. *Lab Chip* **2010**, *10*, 30–35.
- (17) Dias, A. F.; Dernick, G.; Valero, V.; Yong, M. G.; James, C. D.; Craighead, H. G.; Lindau, M. *Nanotechnology* **2002**, *13*, 285–289.
- (18) Berberian, K.; Kisler, K.; Fang, Q.; Lindau, M. *Anal. Chem.* **2009**, *81*, 8734–8740.
- (19) Hafez, I.; Kisler, K.; Berberian, K.; Dernick, G.; Valero, V.; Yong, M. G.; Craighead, H. G.; Lindau, M. *Proc. Natl. Acad. Sci. U.S.A.* **2005**, *102*, 13879.
- (20) Yakushenko, A.; Kätelhön, E.; Wolfrum, B. *Anal. Chem.* **2013**, *85*, 5483–5490.
- (21) Wang, J.; Trouillon, R.; Lin, Y.; Svensson, M. I.; Ewing, A. G. *Anal. Chem.* **2013**, *85* (11), 5600–5608.
- (22) Trouillon, R.; Passarelli, M. K.; Wang, J.; Kurczy, M. E.; Ewing, A. G. *Anal. Chem.* **2013**, *85*, 522–542.
- (23) Gao, Y. F.; Chen, X. H.; Gupta, S.; Gillis, K. D.; Gangopadhyay, S. *Biomed. Microdevices* **2008**, *10*, 623–629.
- (24) Liu, X.; Barizuddin, S.; Shin, W.; Mathai, C. J.; Gangopadhyay, S.; Gillis, K. D. *Anal. Chem.* **2011**, *83*, 2445–2451.
- (25) Meunier, A.; Fulcrand, R.; Darchen, F.; Guille, C. M.; Lemaitre, F.; Amatore, C. *Biophys. Chem.* **2013**, *171*, 84–85.
- (26) Takahashi, Y.; Shevchuk, A. I.; Novak, P.; Babakinejad, B.; Macpherson, J.; Unwin, P. R.; Shiku, H.; Gorelik, J.; Klenerman, D.; Korchev, Y. E.; Matsue, T. *Proc. Natl. Acad. Sci. U.S.A.* **2012**, *109*, 11540–11545.
- (27) Kozminski, K. D.; Gutman, D. A.; Davila, V.; Sulzer, D.; Ewing, A. G. *Anal. Chem.* **1998**, *70*, 3123–3130.
- (28) Mosharov, L. V.; Sulzer, D. *Nat. Methods* **2005**, *2*, 651–658.
- (29) Sombers, L. A.; Hanchar, H. J.; Colliver, T. L.; Wittenberg, N.; Cans, A.-S.; Arbault, S.; Amatore, C.; Ewing, A. G. *J. Neurosci.* **2004**, *24*, 303–309.
- (30) Bond, A. M.; Luscombe, D.; Oldham, K. B.; Zoski, C. G. *J. Electroanal. Chem.* **1985**, *249*, 1–14.
- (31) Strieder, W. *J. Chem. Phys.* **2008**, *129*, 134508.
- (32) Bell, C. G.; Howell, P. D.; Stone, H. A. *J. Electroanal. Chem.* **2013**, *689*, 303–313.
- (33) Trouillon, R.; Lin, Y.; Mellander, L. J.; Keighron, J. D.; Ewing, A. G. *Anal. Chem.* **2013**, *85*, 6421–6428.